Palm-sized Near-Infrared Spectroscopy and Machine Learning Analytics for the Detection of Endogenous Constituents and Drugs in Human Fingernails

Megan Wilson
Pharmacy and Biomolecular Sciences
Liverpool John Moores University
Liverpool, United Kingdom
M.Wilson3@2019.ljmu.ac.uk

Dhiya Al-Jumeily OBE
Computer Science and Mathematics
Liverpool John Moores University
Liverpool, United Kingdom
D.Aljumeily@ljmu.ac.uk

Ismail Abbas
Faculty of Science
Lebanese University
Beirut, Lebonon
ismailabbas057@gmail.com

Iftikhar Khan
Pharmacy and Biomolecular Sciences
Liverpool John Moores University
Liverpool, United Kingdom
I.Khan@ljmu.ac.uk

Jason Birkett
Pharmacy and Biomolecular Sciences
Liverpool John Moores University
Liverpool, United Kingdom
J.W.Birkett@ljmu.ac.uk

Leung Tang
Chemical Analysis Group
Agilent Technology
United Kingdom
Leung_tang@agilent.com

Sulaf Assi
Pharmacy and Biomolecular Sciences
Liverpool John Moores University
Liverpool, United Kingdom
S.Assi@ljmu.ac.uk

Abstract

Near infrared (NIR) spectroscopy offers portable and rapid analysis of endogenous constituents and drugs within fingernails. Fingernails are a useful alternative biological matrix to blood and urine specimen as they provide the advantage of being non-invasive and require minimal sample size (1-3 mm). This work utilised NIR spectroscopy for the detection of (1) drugs in fingernails including benzocaine, calcium carbonate, cocaine hydrochloride (HCl), levamisole HCl, lidocaine HCl and procaine HCl; and (2) endogenous constituents such as carbohydrates, lipids, proteins and water. Fingernails were analysed initially 'as received' to identify the aforementioned endogenous constituents. Seven sets of fingernails were then spiked with one the identified drugs and measured over a six-week period. Spectra were exported into Matlab 2019a for spectral interpretation and machine learning analytics (MLAs). MLAs included correlation wavenumber space (CWS), principal component analysis (PCA) and Artificial Neural Networks Self-Organising Maps (SOM). The results showed that NIR spectra of spiked nails showed key characteristic features at specific wavelengths that corresponded to their spiked drug (1). When combined with CWS and PCA, NIR spectroscopy was able to differentiate between spiked and un-spiked nails and distinguish between the drugs that did not share similar chemical structures. CWS values (r values) and PCA loading scores highlighted spectra/spectral features that were significant. In addition, SOM showed further classes beyond PCA that corresponded to changes in physical properties of the fingernails. Thus, finding confirmed that NIR spectroscopy combined with MLAs possessed the ability to characterise fingernails based on their endogenous constituents and to detect the presence of drugs within fingernails.

Keywords— Fingernails, Drug detection, Cocaine, Near-infrared spectroscopy, Machine learning analytics, Self-organising Maps

I. Introduction

Previously, blood and urine matrices dominated drug testing. However, these specimens offer a short to intermediate window of detection (1-3 days post-consumption) depending on the physicochemical characteristics of the drugs and individuals taking them. Moreover, blood and urine collection methods are often intrusive, invasive, cause donor discomfort and require a trained healthcare worker to conduct. Nonetheless, fingernails are a useful alternative matrix for the detection of endogenous constituents, drugs and metabolites. This is attributed to fingernails accumulating substances over a long period of time and acting as drug depots [1,2]. Substances are incorporated into the fingernails through the blood's simple diffusion process, before they are deposited into the fingernail bed (vertically and horizontally) and the germinal matrix [3].

Previous research successfully identified drugs and metabolites in fingernails including: amfetamine-like stimulants, cocaine and opiates [4, 5]. For example, cocaine metabolite benzoylecgonine has been recorded frequently in fingernails [6]. The detection of metabolites is particularly

useful for drugs such as heroin, which are completely metabolised and leave no parent drug within the bloodstream. In addition to drugs and metabolites, endogenous compounds (carbohydrates, lipids and proteins) have been detected in fingernails [7]. Hence, fingernails provide details regarding the donor's lifestyle, diet, drug/medicine use and disease state.

The NIR region of the electromagnetic radiation (EM) is located at 780 – 2500 nm. NIR spectra offer information regarding the sample's physical properties including particle size, compaction density and polymorphs. This information allows differentiation between samples of the same chemical identity but of different grades/sources. Additionally, the NIR spectra feature both chemical and physical parameters and serves as 'fingerprinting' of measured materials. This makes NIR as a favoured method of choice for rapid and non-destructive detection of drugs, drug impurities and endogenous constituents in fingernails.

The absorbance of NIR spectroscopy is related to overtones and combination bands of molecular vibrations within the mid-IR region of the EM spectrum. NIR principals relate to the theory of an ideal diatomic harmonic oscillator, where vibrational energy in a diatomic molecule results from the bond stretching between two atoms [8]. In the mid-IR region, atoms result in overtones and combinations [9].

$$E \approx (v + 0.5)hf - (v + 0.5)^2 hf\ x$$

Equation 1. The allowed energy levels for an anharmonic oscillator [9].
Where, E is the energy,
h is representative of Planck's constant,
v is the vibrational quantum number,
f represents the equilibrium frequency of oscillation,
x is the anharmonicity constant [9].

NIR spectra are measured in reflectance (*R*) or transmission (*T).* Reflectance is the ratio of radiation intensity that has been reflected by the sample (I_r) to the intensity of the incident radiation (I_0) [11]. *R* in NIR is either specular (surface) or diffuse (after it penetrates sample's particles) and highlights the sample's physicochemical properties (Figure 4) [9].

$$R = I_r I_0$$

Equation 2. Calculation of reflecntace used to measure NIR spectra.
Where, R is reflectance,
I_r is ratio of intensity of radiation reflected by the sample,
I_0 is the intensity of radation impinging on the sample.

Specular radiation, reflected directly from the sample's surface, provides very little information that is useful for identification purposes. However, diffuse radiation, penetrating the sample's core and undergoing multiple reflections, is useful for identification and quantification purposes. Diffuse reflection informs about particle size, particle shape, sample compaction and sample physical state. This study aimed to evaluate the feasibility of handheld NIR spectroscopy alongside machine learning algorithms analytics (MLAs) for detection of drugs, drug impurities and endogenous constituents in human fingernails.

II. Method

A total of 20 participants were recruited via an invitation posted on the Liverpool John Moores University (LJMU) forensic science community site. Those that agreed to take part in the study completed a questionnaire relating to their diet, drug/medicine use and lifestyle, and supplied a fingernail set of 5-10 nails. No identifiable information was sought from participants and anonymity was maintained throughout the study. Each nail set was given an anonymous code and stored in glass vials at room temperature prior to analysis. Ethical approval was provided from two institutions: Liverpool John Moores University (PBS/2021-22/04) and the Lebanese University in Lebanon (2022-0104).

NIR spectra were collected using a palm-sized NIR spectrometer over the wavelength range of 980 – 1670 nm and 100 scans/spectrum, with a total collection of 30 spectra per fingernail set. Prior to analysis, a dark current was taken along with a background using a Spectralon reference standard.

An initial examination took place prior to spiking, this was to identify endogenous constituents including: carbohydrate, lipids and proteins. The glass vial was placed in direct contact with the sample holder).

To investigate the deposition of drugs in fingernails and the ability of NIR spectroscopy to detect drugs, seven sets of fingernails were spiked with cocaine HCl and its adulterants including: benzocaine, calcium carbonate, diltiazem HCl, levamisole HCl, lidocaine HCl and procaine HCl. Approximately 50 mg of the chosen drug was weighed prior to mixing using the SciQuip Vortex VarlMix, which ensured that the fingernails were thoroughly coated for soaking. Fingernails were measured instantly after mixing and up to six-weeks from the date of spiking.

Data collected was exported to Matlab 2019a for spectral interpretation and MLAs application. Spectral pre-treatment was made using multivariate scatter correlation (MSC) and first derivative (D1).

MSC approach was applied to correct offset and baseline in the spectra. MSC corrected the offset of scattered light through the production of a new spectrum that is a linear combination of the original spectrum. This is shown in equation 3 [11].

$$y_{\mathrm{MSC,i}} = \frac{(y_i - a)}{b}$$

Equation 3. Multivariate scatter correlation equation.
Where, $y_{MSC,I}$ is the corrected spectrum value,
y_i is the original spectrum value,
a is the intercept of the line,
and *b* is the slope of the line.

Additionally, *D1* corrected both the offset and baseline of the NIR spectra by using the Savitzsky-Golay method, whereby a second-order polynomial was fitted to the data by least square regression using 13 data points [9]. MLAs applied included correlation in wavelength space (CWS), principal component analysis (PCA) and self-organising maps (SOM).

CWS:

CWS matches the correlation coefficient (r) value of the test spectrum (A) and the reference spectrum (B). Equation 4

demonstrates the calculation of the momentum product (r_p) between spectra A and B.

$$r_p = \frac{\sum(A_i - \bar{A})(B_i - \bar{B})}{\sqrt{\sum(A_i - \bar{A})^2 \sum(B_i - \bar{B})^2}}$$

Equation 4. Correlation coefficient equation based on momentum product.
Where, r_p is the correlation coefficient value corresponding to the momentum product,
A_i is the test spectrum of A,
$\bar{A}$ is the average spectrum of A,
B_i is the reference spectrum of B,
and is the average spectrum of B.

In this respect, an r value of -1 showed that spectra were completely dissimilar, whilst an r value of +1 meant that spectra were identical. Due to instrument and sample noise, obtaining a +1 r value was difficult. Therefore, a threshold of 0.95 was accepted as a pass. Thus, an r value of 0.95 was expected for fingernails spiked with the same drug/drug impurity against each other. An r value of below 0.95 meant that fingernails spiked with different drugs/drug impurities were against each other.

PCA:
In this work, PCA was applied to classifiy spectral data by reducing its dimensionality into two subspaces, those being scores and loadings. The scores highlighted the distribution of spiked fingernails in multidimensional space. The loadings showed significant absorbance values corresponding to significant endogenous constituents within fingernails. The first dimension (PC1) explained the highest variance, the second dimension (PC2) explained the second highest variance, the third dimension (PC3) explained the third highest variance and so on... PC scores were used to identity clusters and patterns within the data set, and to highlight groups of fingernails spiked with similar drugs/drug impurities.
The accuracy of PCA was assessed by the ability to cluster fingernails spiked with the same drug/drug impurity distinct from fingernails spiked with a different drug/drug impurity. PCA models were evalused for type I and type II errors. Type I errors (false negative) occurred when scores of the same fingernail set were not clustered together. Type II errors (false positive) were seen when one score of a fingernail set was clustered with another nail set of different characteristics, for example spiked with a different drug [12].

$$X = T \,.P + \, q$$

Equation 5. PCA equation.
Where, X is the original data matrix (m x P),
T is representative of the scores (m x n),
P represents the loading (n x p) and is representative of the residuals (m x p) [13].

SOM:
SOM provided additional unsupervised clustering approach to PCA and showed the ability to deal with non-linear data in lower dimensions. A key advantage of SOM is in its ability to detect spectral features without previously knowing spectra's classes/memberships. As a neural network mode, SOM is comprised of organised neurons. The output of SOM includes a similarity map of the input data (239 samples and 125 elements) but of lower dimensions. SOM were applied to the data, three variations among the data were expected including: the fingernail's physical properties, the fingernail's water content and the deposition of cocaine, therefore a 3 x 3 SOM was applied. For this chosen method, 100 epoch were trained. Equation 5 demonstrates a classical vector quantisation, which is similar to the mapping in SOM.

$$X = \{\varepsilon_1, \varepsilon_2, \ldots, \varepsilon_j\}^T \mathbb{R}^n$$

Equation 5.
Where, X is the input vector that is real,
ε are the input variables,
j is the number of variables
$\mathbb{R}$ is a set of real numbers.

A parametric real vector (weight) is assigned to each input variable as per equation 6:

$$w_i = [w_{i1}, w_2, \ldots, w_{in}]^T \in \mathbb{R}^n$$

Equation 6.
Where, w_i is the parametric real vector linked to neuron I on the grid and N is the total number of neurons.

If the distance between x and m is d (x, m_i), then the image of the input vector is defined by the array element c that best matches x. This is shown in equation 7.

$$c = \text{argmin}i\{\{d(x, wi)\}$$

Equation 7.

Respectively, c is optimised so that w is close to x and the weight of the winning neuron and its neighbour is updated using equation 8. This occurs until the map converges.

$$v\,(t) = \text{arg}mink\, \epsilon\, \Omega\, \|\varkappa(t) - wk(t)\|$$

$$\Delta wk(t) = \propto(t)n(v,\, k,\, t)[x(t) - wv(t)]$$

Equation 8.
Where,N (v, k, t) is the neighbouring function,
x(t) is the input of time *t,*
$w_v(t)$ is the weight of the winning neuron at time *t.*

III. RESULTS AND DISCUSSION

A. Advantages of NIR spectroscopy

NIR spectroscopy has emerged over the last two decades as a non-destructive and rapid technique for analysis of medicines, drugs and biological samples. For this reason, NIR was chosen to study the deposition of drugs in fingernails. Three MLAs were explored for the identification of drugs within fingernails, including: CWS, PCA and SOM. Fingernails are comprised of a laminated keratinised structure of alpha keratin [14]. Keratins are a group of structural fibrous proteins that are often found in ectodermal tissues, hair, nails and epidermis [15]. Unlike other structural proteins, such as collagen and elastin, keratin possesses sulphur-rich amino acids, cysteine, and disulfide links. These links are present between the cysteine residues and form cystine [16]. Therefore, drugs such as cocaine HCl, which possessed an OH group key for protein binding, yielded a greater affinity for the fingernails' proteins. The

concentration of the drug also played a crucial role in its deposition. Those that are chronically exposed to drugs are more likely to show a higher concentration deposited within the fingernail, which creates greater drug-protein interactions. Thus, individuals who are chronically exposed to drugs, for example drug dealers, are more likely to have greater amount of drugs deposited within their fingernails. This can be detected through NIR spectroscopy and is advantageous for court dealings of possession with intent to supply. Drugs, such as benzocaine, diltiazem HCl, levamisole HCl, lidocaine HCl, and procaine HCl, did not have this imperative OH group and displayed minimum affinity to the fingernails' proteins.

The weak signal of NIR spectroscopy made this technique ideal for non-destructively characterising physical properties of spiked fingernails. This meant that spiked fingernails could be measured 'as received' with no sample crushing or using solvents.

B. NIR spectral interpretation of fingernails

Although NIR spectral interpretation is difficult and based on comparison of samples against reference libraries, it showed ideal in the present study. Hence, fingernails showed important bands related to aliphatic C-H, aromatic/alkene C-H, amine N-H and O-H [17,18]. Therefore, featured wavelengths have been identified to establish functional groups related to fingernails and/or drug(s).

To differentiate endogenous constituents from deposited drugs, previous research was explored. Within the NIR region of 1400 – 1550 nm, water bands are observed. This region is broad, therefore there is some overlap with keratin at 1500 nm. This region is composed of a combination of asymmetric and symmetric OH stretching [19]. Additionally, the proteins within this area are a mixture of C-H vibrations and first overtone N-H. Together protein and water create a broad feature at 1500 – 1530 nm, which is attributed to the overlap of bands created from the strong hydrogen bonds between water and keratin.

Previous research has highlighted that benzocaine and lidocaine HCl were verified within the region 1400 – 1600 nm, as these drugs possessed characteristic N-H functional groups [20]. Benzocaine showed significant band at 1043 nm and this corresponded to the second overtone of the N-H group, associated with a primary amine [21]. Benzocaine, cocaine HCl, levamisole HCl, lidocaine HCl and procaine HCl showed featured wavelengths at 1143 nm (C-H stretch second overtone) related to their aromatic structure, 1180 nm (C-H stretch second overtone) related to their CH_3 group, 1000 – 1100 nm (second overtone) related to their N-H group and 1400 – 1600 nm (region first overtone) related to N-H and O-H groups [20]. Regions characteristic to diltiazem HCl, included 1680 – 1900 nm and 1200 – 1350 nm, which were the results of C-H stretching and S-H stretching in the first and second overtones, respectively. Research has also made clearly a strong connection between calcium carbonate and band at 2338 nm. However, due to limited spectral range of the palm-sized NIR spectrometer, this peak was not detected.

C. CWS

CWS offered an advantage over other MLAs in not requiring numerous spectra for comparison. Hence, only one spectrum was required for each sample (Figure 1). In this respect, the average spectrum for each spiked set was compared against other spiked sets and un-spiked set. Each set showed an r = 0.9999 against itself and that indicated no type I error. However, not all NIR spectra of different sets showed r < 0.95 against each other and that indicated type II errors for mismatches. Hence, nails spiked with lidocaine HCl showed r = 0.98 against nails spiked with procaine HCl. The same r values were obtained for nails spiked with cocaine HCl and diltiazem HCl. This could be attributed to similar chemical characteristics among the aforementioned drugs.

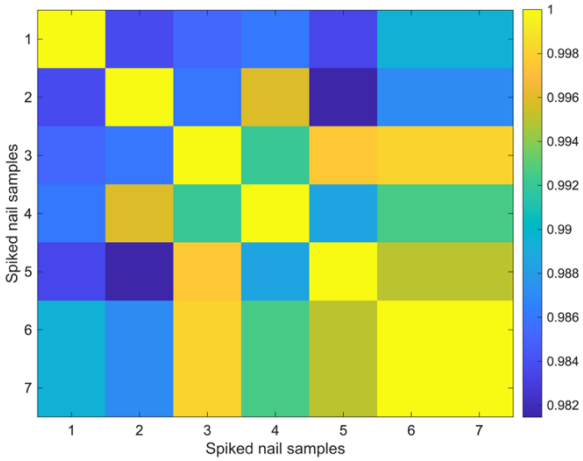

Figure 1. CWS map of the average MSC-D1 NIR spectra of nails spiked with 1) Benzocaine, 2) Calcium carbonate, 3) Cocaine HCl, 4) Diltiazem HCl, 5) Levamisole HCl, 6) Lidocaine HCl, and 7) Procaine HCl and measured using a palm-sized NIR spectrometer.

D. PCA

PCA showed more accurate identification than CWS. Hence, when PCA was applied to the NIR spectra of nails spiked with drugs (over the full range), clusters corresponding to similarities in the structures among the spiked drugs were seen. Figure 2 shows the PC scores plot of the fingernails NIR spectra with adjacent clusters for lidocaine HCl and procaine HCl. This is attributed to drugs sharing similar chemical properties such as benzene and amide groups, which NIR paired with PCA was not able to differentiate between. Yet, the PC scores plots showed distinct clusters for each spiked fingernail that were differentiated from the un-spiked fingernails.

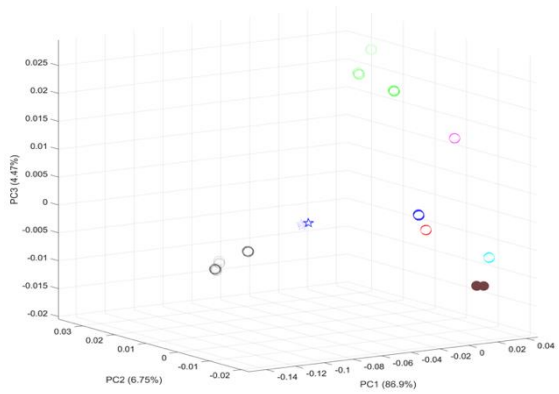

Figure 2. PC scores plot of spiked nails using the palm-sized NIR spectrometer. Fingernails spiked with benzocaine (black circle), calcium carbonate (brown circle), cocaine HCl (green circle), diltiazem HCl (cyan circle), levamisole HCl (magenta circle), lidocaine HCl (blue circle), procaine HCl (red circle), and un-spiked fingernails (blue star).

In this respect, the first three PCs contributed to 98.1% of the variance among the spectra as follows: PC1 86.9%, PC2 6.75% and PC3 4.47%. The PC loading plots showed that PC1 loading corresponding to two main regions being 100 – 1300 nm (C-H 2nd overtone) and 1650 nm ($CHCl_3$) (Figure 3) [9]. PC1 loading had minimal contribution from water (1400 nm) in comparison to PC2 and PC3 loading. Hence, absorbance intensity for water was -0.03 and 0.27 for PC1 and PC2 loadings, respectively. This could be attributed to the OH group present within cocaine that possesses a high affinity to the nail's protein.

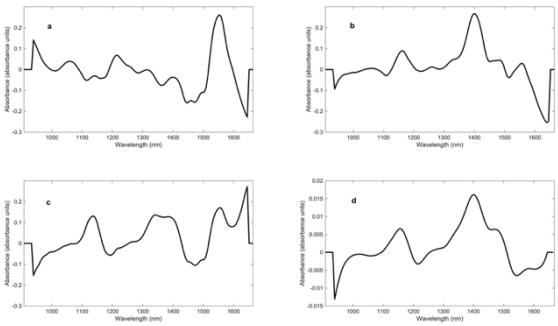

Figure 3. (a) PC1 loading, (b) PC2 loading, (c) PC3 loading and (d) un-spiked fingernail using the palm-sized NIR spectrometer.

E. SOM

SOM showed more detailed clustering when compared to PCA. The U-Matrix showed the weight distances that expressed the distance between neighbouring neurons. Neurons highlighted in Figure 4 were connected to one another by red lines, which showed the distance between neurons. Smaller distances possessed higher densities, while larger distances had lower densities.

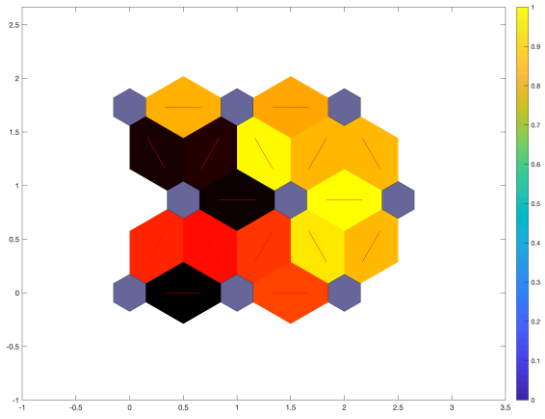

Figure 4. U-Matrix for spectra of spiked fingernails.

In this respect, SOM findings complemented PCA outcomes in further identifying five groups, the first being nails spiked with benzocaine (Figure 5). Fingernails spiked with benzocaine were separated into two groups (group one n = 17, group two n =13) and this was related to the changes benzocaine made to the fingernail's structure. Having benzocaine as two separate clusters indicated type I error. This error could be attributed to NIR measuring diffuse reflectance as well as surface reflectance, therefore information is taken from the surface and the inside of the fingernail. This may create inconsistencies in physical properties and must be confirmed using confocal microscopy. A second group (n = 30) comprised of un-spiked fingernails that were clustered distinctly in PCA and SOM. The third identified group (n = 60) corresponded to fingernails spiked with calcium carbonate and diltiazem HCl. Cocaine HCl and levamisole HCl made up the fourth group (n = 60). This can be attributed to a type II error, whereby two different sets of spiked fingernails have been grouped together despite not sharing any chemical similarities. The final group (n = 59) consisted of fingernails spiked with lidocaine HCl and procaine HCl. As previously mentioned, this is attributed to lidocaine and procaine sharing similar chemical structures.

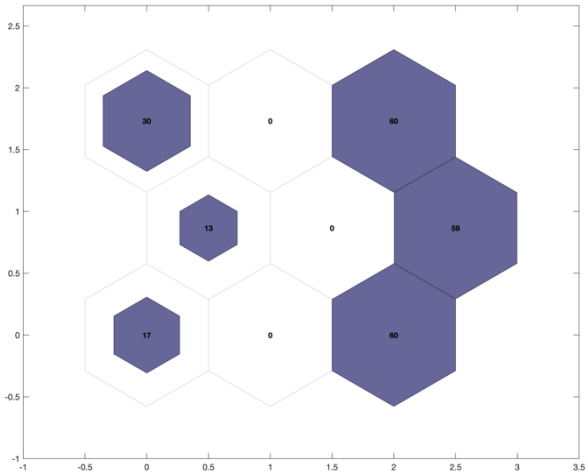

Figure 5. Sample hit map for spectra of spiked fingernails.

IV. Conclusion

This work evaluated feasibility of NIR spectroscopy for rapid and non-destructive detection of drugs deposited into

fingernails. Furthermore, NIR offered the advantage of a weak signal, which makes it an ideal technique for characterising physiochemical properties of drugs deposition within fingernails. The non-destructive nature of NIR allowed fingernails to be measured 'as received' without crushing, changing morphology or extensive sample preparation. However, the weak NIR signals produced overlapping spectra, which required data-treatment and the use of MLAs. MLAs applied to NIR spectra were complimentary for characterising drugs in fingernails. CWS, PCA and SOM were successful in classifying different sets of spiked fingernails. CWS analysis was advantageous as it required a minimal number of collected spectra for the comparison of r values. Whereas, PCA required a greater number of spectra to ensure accuracy and a sufficient level of variance. Therefore, PCA showed detailed information corresponding to the samples' physical characteristics. For such analytics to be employed in future casework, multiple fingernail samples must be collected in the form of fingernails clippings. This is attributed to PCA analysis requiring a large sample size.

Ultimately, this research showed that NIR spectroscopy paired with MLAs were effective at identifying drug deposition in fingernails after a period of six weeks. Additionally, this has allowed for the development and validation of a NIR spectroscopic library for future analysis.

Future work will include the addition of a complimentary technique to NIR, such as Raman and/or infrared spectroscropy. Both techniques have the ability to produce information regarding a sample's chemical characteristics. Thus, will make suitable complimentary techniques for NIR spectroscopy for detection of drugs, drug impurities and endogenous constituents in fingernails.

V. REFERENCES

[1] Cappelle, D., De Keukeleire, S., Neels, H., Been, F., De Doncker, M., Dom, G., Crunelle, C., Covaci, A. and van Nuijs, A. (2018). Keratinous matrices for the assessment of drugs of abuse consumption: A correlation study between hair and nails. Drug Testing and Analysis, 10 pp.1110-1118 DOI: 10.1002/dta.2356 [Accessed 20th October 2022].

[2] Cappelle, D., Yegles, M., Neels, H., van Nuijs, A., De Doncker, M., Maudens, K., Covaci, A. and Crunelle, C. (2014). Nail analysis for the detection of drugs of abuse and pharmaceuticals: a review. Forensic Toxicology, 33 pp.12-36 DOI: 10.1007/s11419-014-0258-1 [Accessed 20th October 2022].

[3] Hill, V., Stowe, G., Paulsen, R. and Schaffer, M. (2018). Nail Analysis for Drugs: A Role in Workplace Testing?. Journal of Analytical Toxicology, 42 pp.425-436 DOI: 10.1093/jat/bky020 [Accessed 20th October].

[4] Engelhart, D. and Jenkins, A. (2002). Detection of Cocaine Analytes and Opiates in Nails from Postmortem Cases. Journal of Analytical Toxicology, 26 pp.489-492 DOI: 10.1093/jat/26.7.489 [Accessed 20th October].

[5] Susa, S. and Preuss, C. (2021). Drug Metabolism. 1st ed. Treassure Island, Florida: StatPearls Publishing.

[6] Garside, D., Ropero-Miller, J., Goldberger, B., Hamilton, W. and Maples, W. (1998). Identification of Cocaine Analytes in Fingernail and Toenail Specimens. Journal of Forensic Sciences, 43 pp.14344-14345.

[7] Gomez-Gomez, A., Montero-San-Martin, B., Haro, N. and Pozo, O. (2021). Nail Melatonin Content: A Suitable Non-Invasive Marker of Melatonin Production. International Journal of Molecular Sciences, 22 pp.921-922.

[8] Zoppi, M. (1993). Neutron scattering of homonuclear diatomic liquids. Physica B: Condensed Matter, 183 pp.235-246.

[9] [NIR Spectroscopy]. [RD Jee]. In: Moffat AC, Osselton MD, Elliott SP (eds). Clarke's Analysis of Drugs and Poisons, [online]. London: Pharmaceutical Press. http://www.medicinescomplete.com/ [Accessed 20th October 2022]

[10] Moraes, L., Rocha, R., Menegazzo, L., Araújo, E., Yukimito, K. and Moraes, J. (2008). Infrared spectroscopy: a tool for determination of the degree of conversion in dental composites. Journal of Applied Oral Science, 16 pp.145-149.

[11] K. Varmuza, P. Filzmoser, Introduction to multivariate statistical analysis in chemometrics. CRC press (2016).

[12] Assi, S, Arafat, B, Lawson-Wood, K and Robertson, I (2020). Authentication of Antibiotics Using Portable Near-Infrared Spectroscopy and Multivariate Data Analysis. Applied Spectroscopy, 75(4), pp.434-444.

[13] Jolliffe, I. and Cadima, J. (2016). Principal component analysis: a review and recent developments. Philosophical Transactions of the Royal Society A: Mathematical, Physical and Engineering Sciences, 374 (2065), pp.1-4 DOI: 10.1098/rsta.2015.0202 [Accessed 20th October 2022]

[14] De Berker, D., Wojnarowska, F., Sviland, L., Westgate, G., Dawber, R. and Leigh, I. (2000). Keratin expression in the normal nail unit: markers of regional differentiation. British Journal of Dermatology, 142 pp.89-96.

[15] Bragulla, H. and Homberger, D. (2009). Structure and functions of keratin proteins in simple, stratified, keratinized and cornified epithelia. Journal of Anatomy, 214 pp.516-559.

[16] Baraldi, A., Jones, S., Guesné, S., Traynor, M., McAuley, W., Brown, M. and Murdan, S. (2014). Human Nail Plate Modifications Induced by Onychomycosis: Implications for Topical Therapy. Pharmaceutical Research, 32 pp.1626-1633.

[17] Fontalvo-Gómez, M., Colucci, J., Velez, N. and Romañach, R. (2013). In-Line Near- Infrared (NIR) and Raman Spectroscopy Coupled with Principal Component Analysis (PCA) for in Situ Evaluation of the Transesterification Reaction. Applied Spectroscopy, 67 pp.1142-1149 DOI: 10.1366/12-06729 [Accessed 20th October 2022]

[18] Pevelen, D.L. and Tranter, G. (2017). Encyclopedia of Spectroscopy and Spectrometry. 3rd ed. Amsterdam: Elsevier.

[19] Feng, Z., Tang, T., Wu, T., Yu, X., Zhang, Y., Wang, M., Zheng, J., Ying, Y., Chen, S., Zhou, J., Fan, X., Zhang, D., Li, S., Zhang, M. and Qian, J. (2021). Perfecting and extending the near-infrared imaging window. Light: Science & Applications, 10 pp.5-6.

[20] Correia, R., Domingos, E., Tosato, F., dos Santos, N., Leite, J., da Silva, M., Marcelo, M., Ortiz, R., Filgueiras, P. and Romão, W. (2018). Portable near infrared spectroscopy applied to abuse drugs and medicine analyses. Analytical Methods, 10 pp.593-603 DOI: 10.1039/c7ay02998e [Accessed 20th October 2022]

[21] Workman, J. (2006). Interpretive Spectroscopy for Near Infrared. Applied Spectroscopy Reviews, 31 pp.251-320.